Lingacom Muography

A. Harel   D. Yaish

May 2018

Abstract

Lingacom Ltd. develops detectors for muography – imaging using cosmic-ray muons, together with imaging algorithms and tools. We present selected simulation results from muon imaging of cargo containers, from a joint muon and X-ray imaging algorithm, and for ground surveys using borehole detectors. This follows a presentation in the "Cosmic-ray muography" meeting of the Royal Society.

1 Lingacom Ltd.

Lingacom Ltd. specializes in imaging using cosmic-ray muons. We aim to commercialize a patented, state-of-the-art suite of detection solutions built on our proprietary muon-based detectors, algorithms, and imaging technology. We seek to provide our customers with unprecedented 3D imaging capabilities for homeland security and underground mapping and to improve the detection coverage, false-positive rates and form factors of detection systems for civil engineering, mineral exploration and homeland security. Lingacom Ltd. is a privately-held Israeli company, founded in 2012 by experienced information-technology executives and entrepreneurs D. Yaish and Y. Kolkovich.

The target markets are inspection of cargo and vehicles, and underground mapping. Cargo and vehicle inspection is geared [1] towards the detection of special nuclear material (SNM). The inspection can occur at sea ports, border crossings, air ports, or at sensitive sites such as nuclear power plants. Some of the potential usages of underground mapping are in the mining industry [2], specifically in mineral exploration, and in the field of civil engineering (see Fig. 1).
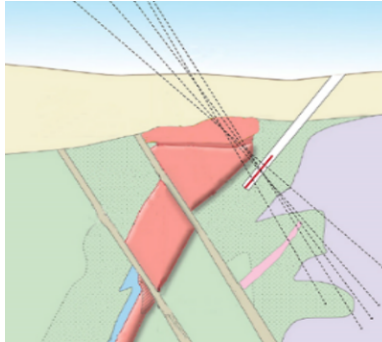
Figure 1: Usage scenario for a bore hole detector in mapping a mineral deposit.

Our products are gaseous-amplification ionizing-particle detectors and imaging tools. Our detector technology can be implemented in various form factors and spatial resolution, to fit various usage scenarios. This includes optimizations for the rate of cosmic-ray muons (CRMs), which is much lower than the rates encountered in particle accelerators, the environment for which most gaseous-amplification ionizing-particle detectors were developed. Our detector technology addresses several design and production challenges to allow us to operate our gas detectors in sealed mode, which greatly simplifies the overall system and reduces the operational costs for our customers. Figure 2 shows the setup of a test for long-term stability of a simple detector prototype, with some results shown in Fig. 3.

Figure 2: A simple gas detector prototype used in the stability test. Additional fast ionizing-particle "trigger" detectors used to confirm well-timed signals from the gas detector are located below the desk and are not visible in this photo.

We implement our detector technology in flat detectors, as suitable for hodoscopes, cargo imaging systems, and some mining scenarios, and in borehole detectors for civil engineering applications. Prototypes of both types of
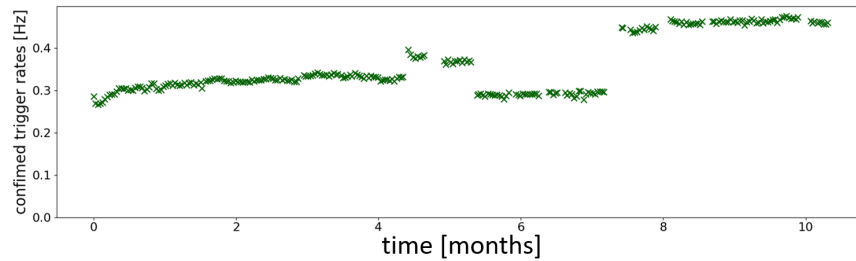
Figure 3: The rate of confirmed triggers from the sealed gas detector of Fig. 2 as a function of time. The sudden jumps in rates are due to changes in the location of the stability test setup and to changes in the location of the gas detector relative to the trigger detectors.

detectors are shown in Fig. 4.

Figure 4: Lingacom detectors.

2 Detection of Shielded Nuclear Materials in Dense Containers

Current scanning tools available at border crossing, and in particular in sea ports where vast quantities of container pass through, are unable to detect SNM in dense cargo. Sufficient shielding of the nuclear material, for example by a lead sheathing or by placement within a large iron structure, lowers the rate of emitted radiation so that simpler counting detectors do not identify the presence of nuclear materials. Another powerful scanning tool used at border crossing is X-ray scanning, using high-energy (e.g. 5 MeV to 10 MeV) X rays. The SNM shows up in the X-ray images as a dark impenetrable block. However such blocks appear in a sizable fraction of containers due to ordinary dense cargo. Lingacom Ltd.'s inspection solutions focus on such

dense containers. Here are below we discuss containers, however the discussion also holds for vehicles scanned at border crossing, entrances and exits from sensitive sites, etc.

The basic concept of operation of the Lingacom solutions is to use an X-ray imaging system as a primary detection system and a CRM imaging system as a secondary detection system. Naturally other detection techniques in current use, such as radiation portal monitors (RPMs), still have their roles. The primary X-ray system can clear most containers, allowing for a high throughput of the combined system. When the X-ray system encounters a dense area in a container it passes the container to the muon system. The container is then placed so that the dense area is in the middle of the volume scanned by the muon system (see Fig. 5), and this part of the container is imaged. The muon system can clear most dense containers, reducing the need for the labor-intensive task of unpacking the container, manually inspecting its content, and repacking it.
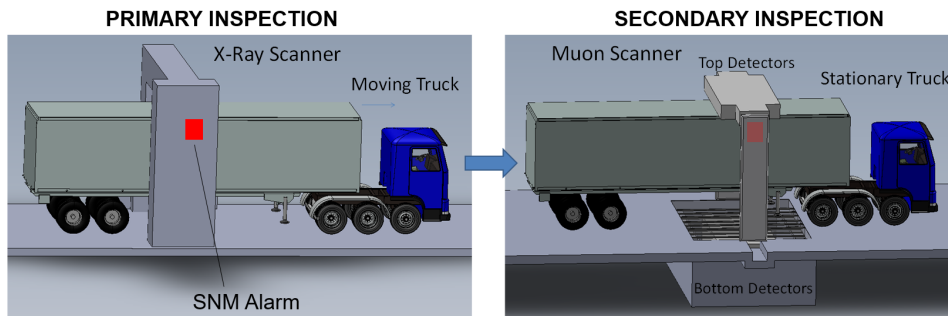

Figure 5: Concept of operations — an X-ray scan serves as a primary system and dense cargo is passed to a muon scanner serving as a secondary system.

The main components of the muon system are flat CRM detectors, which are arranged in layers. There are two layers above the scanned cargo, which measure the direction and location of the incoming muons, and two more layers below the scanned cargo, which measure the exit direction and location of the muon. From these observables, each muon's angular and spatial deflections are calculated. With the usual approximation [3, 4], the width of the distribution of deflections (σ) through a segment of length L is roughly

$$\sigma \approx \frac{\sqrt{\lambda L}}{\beta p},\tag{1}$$

4

where p is the muon's momentum and β is the muon's velocity in natural units[1]. This implies that the muon's momentum determines the scale with which we should interpret a muon's scattering as "big" or "small". As demonstrated in Table 1, the differences in σ due to realistic variations in the muon's momentum are far larger than the differences due to the material being traversed. The muon system includes a spectrometer, located just below the four layers detailed above (see Fig. 6). This design is tailored to the spatial resolution of our detectors. In particular, in the use of scattering layers and in the optimization of the spacing between the layers. Lingacom uses proprietary algorithms to reconstruct the muon's momentum and for the 3D muon imaging of the scanned volume.

Table 1: Muon scattering with (in milliradians) for selected muon momenta – adapted from Ref. [4]

Material	$p = 0.3\,\mathrm{GeV}$	$p = 3\,\mathrm{GeV}$	$p = 30\,\mathrm{GeV}$
Water	26.3	2.6	0.3
Concrete	48.3	4.8	0.5
Iron	119.2	11.9	1.2
Lead	211.3	21.1	2.1
Uranium	279.5	28.0	2.8

Lingacom developed a unique, proprietary imaging algorithm that uses both the X-ray image from the primary system and the muon data from the secondary system to reconstruct the 3D scattering density map of the scanned volume. The algorithm is based on a physical model that captures the main features of the correlation between muon scattering and X-ray absorption. The potential of this algorithm is demonstrated in Fig. 7. In this test bench, adding the X-ray data improved the signal-over-noise ratio by a factor of ≈ 3, from 2.2 to 6.7.

3 Case Studies for Underground Mapping

In underground usage, muon absorption is used rather than muon scattering. For muons of the relevant energies ($0.3\,\mathrm{GeV}$ to $\approx 50\,\mathrm{GeV}$ for civil engineering),

---

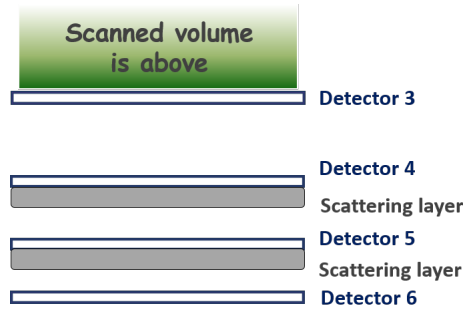[1]Often this is further approximated by dropping the β term.

Figure 6: Main components of the muon inspection system below the scanned volume. The spectrometer comprises the scattering layers and detection layers 5 and 6.
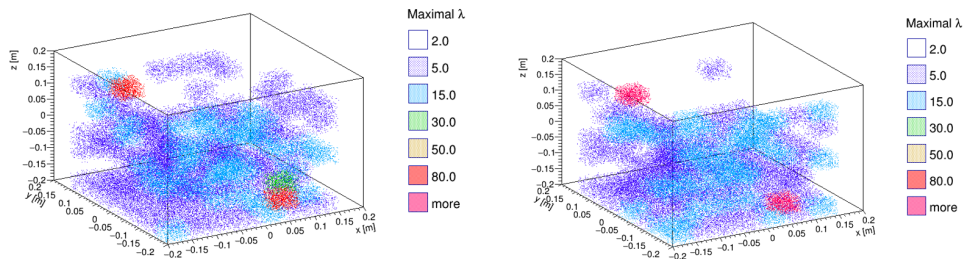

Figure 7: Reconstruction results for a simulated test scenario. The image from muon-only data is on the left; the image from the joint reconstruction is on the right. The scanned volume containing a $(40\,\mathrm{cm})^3$ aluminum block in which two $(5\,\mathrm{cm})^3$ blocks of Uranium are embedded.

the small dependence of muon energy loss on the chemical composition of the traversed material and the limited variety in chemical compositions of rocks and soils combine so that the rate of muon absorption depends almost entirely on the integrated mass-density (or "opacity" [5]) of the ground along its path. As the muons slow down gradually in their passage through the ground[2], any muon that reaches the detector had a large energy earlier in its path, and thus little scatter (as discussed above). Thus most of the angular scatter of each muon occurs in the last few meters before reaching the detectors (see further discussions in Ref. [5]), and results in a uniform smearing of any image. This smearing is sufficiently small and uniform that the angular scattering can be ignored during the imaging, and we will do so in what follows. Thus a measurement of the CRM flux in some angular area (e.g. an elevation angle α of 40° to 45° and an azimuthal angle ϕ of 0° to 5°) can be translated to a measurement of the opacity in that direction.

The active area of borehole detectors is severely limited by the available space. Thus long exposure times might be necessary to detect an irregularity or to image the underground densities. We report here two case studies of the required exposure times to detect ground-density anomalies using the borehole detectors described above. In these case studies we use only simple per-detector 2D images. The image for each detector is constructed by binning the muons detected at the detector by their incoming direction. Furthermore, some knowledge of the expected muon counts is assumed, with systematic uncertainties equal to the statistical uncertainties in the measurement itself.

In practice, a 3D image will be formed by combining the data from several detectors in several boreholes. Though this imaging problem is superficially similar to the text book "inverse problem" for X-ray absorption in tomography, in muography the statistical uncertainties due to the limited CRM flux dominate, and somewhat different algorithms are useful (see References [6], [7], and [8] for various approaches).

The first use case is to locate a large sewer pipe. This arises when a building site is prepared for a dig and the pipe is not found in the expected location. We take the pipe diameter to be 1.5 m, its depth to be 2 m, and allow it to be a third full with water. We take the ground density to be 1.7 gcm^{-3}. The coverage provided by a pair of detectors, located 7 m apart at a depth of 5 m is shows in Fig. 8.

_____

[2]We use the term "ground" to refer to rocks, soils, and man-made objects present in the underground volume being imaged.
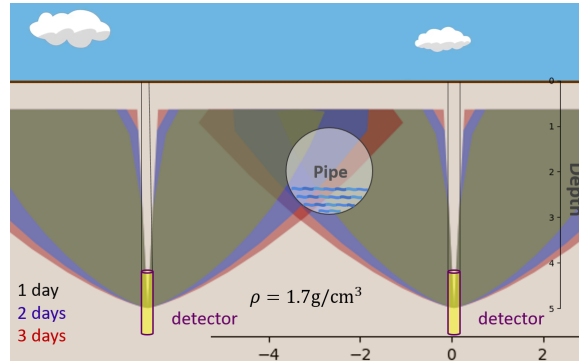
Figure 8: Calculated coverage areas for various exposures for the sewer pipe use case. The shading at each location indicates the required exposure time to detect the sewer pipe if it is centered on that location.

The second use case is to locate a large karst cavity in rock. We take the cavity dimensions to be $(25\,\text{m})^3$ and its depth to be $32.5\,\text{m}$. We take the rock density to be $2.3\,\text{gcm}^{-3}$. The coverage provided by a borehole detector located at a depth of $60\,\text{m}$ is shows in Fig. 9.
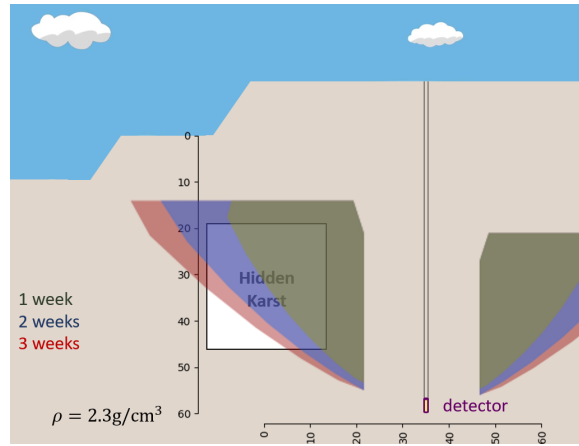

Figure 9: Calculated coverage areas for various exposures for the karst use case. The shading at each location indicates the required exposure time to detect the cavity if it is centered on that location.

Both authors contributed to all the work detailed here and to the manuscript. Both authors read and approved the manuscript. D. Yaish is the CEO and

References

[1] For example, Borozodin KN. *et al.* 2003 Radiographic imaging with cosmic-ray muons *Nature* **422**; or
Riggi S. *et al.* 2013 Muon tomography imaging algorithms for nuclear threat detection inside large volume containers with the Muon Portal detector *Nucl. Intrum. and Meth. in Phys. Res. Sec. A* **728**.

[2] For example, Bryman D. *et al.* 2014 *Muon Geotomography — Bringing New Physics to Orebody Imaging.* Society of Economic Geologists, Inc.: Special Publications **18**.

[3] Rossi, B. 1952 *High Energy Particles.* Prentice-Hall, Inc., Englewood Cliffs, NJ.

[4] Schultz, LJ. 2003 *Cosmic Ray Muon Radiography.* Ph.D. Thesis, Portland State University.

[5] Lesparre N., Gibert D., Marteau J., Déclais Y., Carbone D., and Galichet E. 2010 *Geophysical muon imaging: feasibility and limits.* Geophys. J. Int. **183**.

[6] Davis K. *et al.* 2011 *Joint 3D inversion of muon tomography and gravity data.* Proceedings of the International Workshop on Gravity, Electrical & Magnetic Methods and their Applications. The Society of Exploration Geophysicists and the Chinese Geophysical Society.

[7] Jourde K., Gibert D., and Marteau J. 2014 *Joint inversion of muon tomography and gravimetry - a resolving kernel approach.* Geosci. Instrum. Method. Data Syst. Discuss., **5**.

[8] Guardincerri E. *et al.* 2017 *3D Cosmic Ray Muon Tomography from an Underground Tunnel* Pure Appl. Geophys. **174**.